Biomedical Signal Processing and Control 57 (2020) 101790

Contents lists available at ScienceDirect

Biomedical Signal Processing and Control

journal homepage: www.elsevier.com/locate/bspc

Heart rate estimation from wrist-type photoplethysmography signals during physical exercise

K.R. Arunkumar*, M. Bhaskar

Department of Electronics and Communication Engineering, National Institute of Technology Tiruchirappalli, Tiruchirappalli 620 015, India

ARTICLE INFO

Article history:
Received 7 August 2019
Received in revised form 6 November 2019
Accepted 16 November 2019
Available online 26 December 2019

Keywords:
Photoplethysmography
Combination of RLS, NLMS and LMS adaptive filters
Softmax activation function
Motion artifact
Fast Fourier transform
Phase vocoder
Heart rate estimation

ABSTRACT

Wearable devices, such as smart watch use photoplethysmography (PPG) signals for estimating heart rate (HR). The motion artifacts (MA) contained in these PPG signals lead to an erroneous HR estimation. In this manuscript, a new de-noising algorithm has been proposed that uses the combination of cascaded recursive least square (RLS), normalized least mean square (NLMS) and least mean square (LMS) adaptive filters. The MA reduced PPG signals obtained from these cascaded adaptive filters are combined using the softmax activation function. Fast Fourier transform (FFT) is used to estimate the HR from the MA reduced PPG signals and phase vocoder is used to refine the estimated HR. The performance of the proposed method in the form of mean error, standard deviation of the mean error and mean relative error is analyzed using the 22 datasets given for IEEE Signal processing cup 2015. This resulted in an error of 1.86 beat per minute (BPM) tested on 22 datasets which is less compared to other existing methods.

1. Introduction

Photoplethysmography used in wearable devices is simple, non-invasive, low-cost optical technique that estimates human parameters like oxygen saturation, HR, blood pressure, etc. [1]. Due to its non-invasive property, it is widely used in commercially available wearable devices. Even though wearable devices show promising development in health care, reliability and effectiveness in estimating the human health parameters is of significant concern [2]. The wearable devices used to estimate HR is highly challenging [3]. Electrocardiogram (ECG) which estimates the HR more accurately is not convenient to be used in wearable devices, especially during body movement because more wires are to be attached to the skin for signal acquisition. PPG is used in wearable devices to estimate the HR because it is highly comfortable than the conventional ECG, as it is not glued to the skin [4]. The PPG signal obtained via the PPG sensors, are integrated in wearable devices. The PPG sensors emit light to the skin and the variation in the intensity of the light that is transmitted or reflected through the skin is sensed by the photo diode (PD) [5]. The light emitted from PPG sensor is green in color and its wavelength is 515 nm [6]. The PPG sensors placed in the finger [7] transmits the light through the skin and collects the transmitted light at PD. The PPG sensors and PD face each other. This is called transmission type [8]. Similarly, the PPG sensors placed at forehead [9] and wrist transmit the light to the skin and collect back the reflected light at PD. This is called reflectance type [10]. In this type, the PPG sensor and PD are placed on the same side. HR estimated from the wrist through PPG sensors is challenging because the wrist movement results in the movement of the PPG sensors as well as the tissues thereby corrupting the PPG signal by the addition of MA, a type of noise generated due to body movement [11].

All the works that have so far been reported for estimating the HR from the wrist type PPG involve three stages: de-noising, HR estimation, and tracking. Different de-noising techniques for removing MA from PPG signal have already been proposed. The HR estimated from Troika method used singular spectrum analysis, a signal decomposition technique for de-noising, sparsity based spectrum estimation for HR estimation, spectral peak tracking and verification for HR tracking. The Troika method recorded an error of 2.73 beat per minute (BPM) on 22 recorded PPG signals [12]. However, the signal decomposition technique used in Troika failed to estimate the HR accurately. To subjugate this drawback, joint sparse spectral reconstruction (JOSS), an enhancement of Troika method has been proposed [13]. In JOSS, the spectral sparsification and spectral subtraction method for de-noising and spectral

* Corresponding author.
E-mail address: arunrameshwaran@gmail.com (K.R. Arunkumar).

https://doi.org/10.1016/j.bspc.2019.101790
1746-8094/

peak tracking and verification for HR estimation and tracking has been reported. The error reported for JOSS on 22 PPG recordings was 2.08 beat per minute (BPM). JOSS has an issue in estimating the HR when MAs were strong at the initial stage. In [14,15], de-noising was performed using Wiener filter and phase vocoder was used for estimating the spectral peak and refining it and was followed by HR tracking. An error of 1.90 beat per minute (BPM) on 22 PPG recordings was reported [14]. Kalman filter based de-noising technique was used in [16] to reduce the influence of MA from PPG signal that resulted in an error of 1.99 beat per minute (BPM) on 22 PPG recordings. Sub-space decomposition based de-noising, Fourier based HR estimation and Kalman filter based smoothening and tracking were reported in [17] and an error of 2.45 beat per minute (BPM) was recorded when tested using 22 PPG datasets.

Adaptive filters are preferred to remove the MA present in the corrupted PPG signal. When the MA spectrum is strong and its spectrum overlap that of PPG spectrum, removing the MA using traditional filter with fixed filter co-efficient will fail to preserve the PPG spectrum as the PPG and MA signals are time-varying in nature. The adaptive filters successfully remove the MA spectrum without affecting the spectrum of PPG signal because the filter co-efficient used in the adaptive filters are updated automatically based on the adaptive algorithm. The adaptive filters do not require any prior information about the PPG signal and MA [18].

The most common application of the adaptive filters is adaptive noise cancellation (ANC). The ANC uses accelerometer signals as reference noise input signal for minimizing MA present in PPG signal [19]. The ANC technique is a tool for estimating the signals corrupted by additive noise. It has a faster response time and it is capable of reducing the in-band noise effectively that are added to the signal [20]. The effective noise reduction depends on the reference noise signal given as an input. In [21], NLMS adaptive filters with PPG1 and PPG2 signals as desired inputs and accelerometer X, Y and Z as reference noise inputs have been proposed. The MA reduced PPG signal was obtained by combining the output of the six NLMS filters, from which the HR was estimated. In [22], RLS adaptive filters with single channel PPG was used as desired input and three axes accelerometer X, Y and Z along with the difference of two PPG channels were used as reference noise inputs. All the design techniques mentioned above are single stage adaptive filters and performs parallel operation. In [23], singular spectrum analysis (SSA) technique was combined with three stage cascaded RLS adaptive filters for de-noising. The average of two PPG channels was given as the desired input and accelerometer X, Y and Z as reference noise inputs. The clean PPG signal corrupted by MA was de-noised by both cascaded adaptive filter structure and SSA technique. Logical combination technique was used to combine these de-noised PPG signal from which HR was estimated. The combination of non-linear adaptive filtering using RLS Volterra and signal decomposition for estimating HR from the PPG signal was proposed in [24]. In [25], the combination of ensemble empirical mode decomposition (EEMD) based signal decomposition technique and three constrained RLS adaptive filters that were cascaded was used for de-noising and HR was estimated using the coupled wavelet-Fourier based technique.

Different structures of adaptive filter like single-stage, multi-stage, cascaded and parallel have already been reported for removing MA from PPG signals. Combining two or more adaptive filters has resulted in robustness, improved tracking ability of time-varying parameters and error value reduction and thereby improving the quality of the output signal [26,27]. Combination of adaptive filters was not explored to the extent to which the conventional adaptive filters were explored. The cascaded adaptive filters were combined for de-noising and estimating the HR [28,29]. Spectral subtraction technique was used to remove the accelerometer spectrum from the PPG spectrum, thereby reducing the MA spectrum from the PPG spectrum [30].

In this paper, a de-noising method for MA removal from PPG signal has been proposed. A new de-noising structure having three-stage cascaded de-noising structure that combines RLS, NLMS and LMS adaptive filters is proposed for MA reduction from the corrupted PPG signal. At the combinational layer, the cascaded RLS, NLMS and LMS adaptive filters output are combined using the combinational parameter λ to form a MA reduced PPG signal, $s[n]$. The combinational layer determines which filter component performs better at each time instant and allocates the weights dynamically based on their performance.

The manuscript is organized as follows. Section 2 describes the PPG dataset used in this work followed by the proposed HR estimation technique and post-processing. Experimental results obtained using this dataset is presented in Section 3 and finally, the conclusion in Section 4.

The major contribution of this paper includes:

- A robust and computationally efficient de-noising technique that combines three stages of cascaded adaptive filters like RLS, NLMS and LMS has been proposed.
- The filtered output obtained from the RLS, NLMS and LMS adaptive filters are combined using softmax activation function.
- The search range (SR), a band of location points from which the HR is estimated, has been selected dynamically by varying the parameter Δ, which depends on the power value of the accelerometer signals.
- The proposed method delivers less error value when evaluated on 22 datasets each performing different activity.

2. Material and method

2.1. Dataset description

The dataset used in this work was provided for IEEE signal processing cup 2015. The dataset has 22 recordings, each of 5 min duration. These recordings were collected from individuals who performed different physical activities and their ages varied from 18 to 58. Each dataset has recordings of PPG1 and PPG2 signals acquired from individual PPG sensors, tri-axes accelerometer signals, namely, accelerometer-X (ACC-X), accelerometer-Y (ACC-Y) and accelerometer-Z (ACC-Z). These signals were recorded from the wrist of 22 individuals. The PPG sensors were separated by 2 cm from each other. The PPG sensors and accelerometer sensors were embedded in the wrist band from which the signals were acquired. The ECG signal was also recorded simultaneously from the chest of each individual using ECG sensors along with the recording of PPG signal and accelerometer signal. PPG signals and the accelerometer signals were sampled at 125 Hz. The 22 datasets were divided into 12 training datasets and 10 testing datasets. The training dataset was obtained from 12 male individuals performing walking and running activity on a treadmill at a maximum speed of 15 km/h. The individuals were told to use the hand together with the wristband to take clothes, wipe sweat on the forehead and press buttons on the treadmill apart from free hand swing motion. The 10 testing datasets were recorded from 8 individuals comprising 7 male and 1 female. The female reported to have an abnormal heart rhythm and blood pressure. These 8 individuals performed vigorous physical activities like hand-shake, stretch, push, running, jump, push-up, boxing, swimming and weight-lifting. The ECG signals were recorded simultaneously provides the ground truth HR in BPM. The HRs estimated from ECG signals were calculated for every 8 s window with 2 s shift. Also, the HR estimated from the PPG sig-

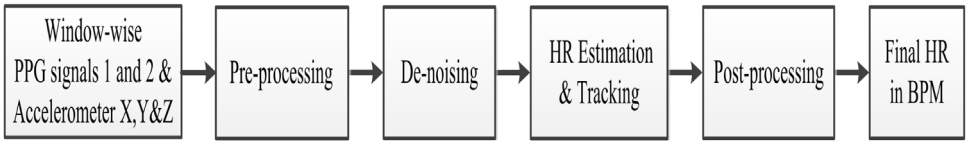

Fig. 1. Block diagram of the proposed de-noising technique for HR estimation.

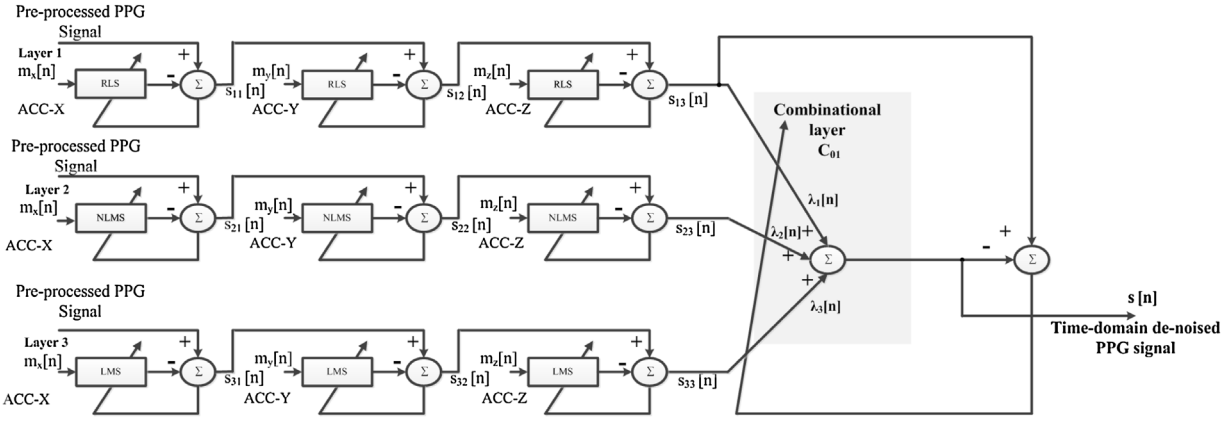

Fig. 2. Combination of RLS, NLMS and LMS adaptive filters for removal of MA.

nals uses the same window length and shift, so that the number of HR estimates and ground truth HRs are same [12,13].

2.2. Proposed HR estimation technique

The block diagram of the proposed HR estimation technique is depicted in Fig. 1. The HR estimated from the proposed method involves the following levels namely, pre-processing, de-noising, HR estimation & tracking and post-processing.

2.2.1. Pre-processing

The PPG signals collected from the PPG sensors are normalized and then averaged. The averaged PPG signal and tri-axes accelerometer signals are transformed to frequency-domain from time-domain using FFT. These frequency-domain signals are passed through a frequency-domain band pass filter. This filter selects the signal of frequency ranging from 0.4 to 3.5 Hz and discards other frequencies. The PPG and tri-axes accelerometer signals from 0.4 to 3.5 Hz (i.e. from 24 to 210 BPM) are alone investigated for the next levels like de-noising, HR estimation & tracking and post-processing. By using inverse fast Fourier transform (IFFT), these filtered signals are transformed back from frequency-domain to time-domain. This time-domain PPG signal is contemplated for the presence of MA and it is removed at the de-noising level itself.

2.2.2. De-noising using combinations of adaptive filters

In this paper, combination of three stage cascaded RLS, NLMS and LMS adaptive filters is proposed for better MA removal and is shown in Fig. 2. Three stage cascaded structure is proposed, because the MA component is spawned due to the body movements which is recorded as the tri-axes accelerometer signals:

$$m[n] = w_x m_x[n] + w_y m_y[n] + w_z m_z[n] \quad (1)$$

where $m_x[n]$, $m_y[n]$ and $m_z[n]$ – tri-axes accelerometer data, w_x, w_y, w_z – weighting parameters, and $m[n]$ – motion artifact.

The three axes accelerometer signal gives information about the MA generated due to body movements. There is a strong correlation between the accelerometer and PPG signals. The MA component of a single accelerometer or the MA components of all the accelerometers may corrupt the PPG signal. This can be realized from Fig. 3, where the MA components generated by ACC-X and ACC-Y corrupts the PPG signal. In Fig. 3a, ECG signal based HR is denoted by pink triangle whereas the HR estimated from PPG signal using the periodogram is indicated by red circle. The original HR and estimated HR differ by ≈40 BPM and this can be seen in Fig. 3a. This is due to the movement of the body in a specific direction and that has been recorded in tri-axis accelerometer signals. The maximum hand movements that occur at a particular HR is identified by red circle as shown in Fig. 3b–d. It is noted from the Fig. 3b and c, the maximum hand movements occur at ≈160 BPM which has a huge influence on HR estimation of the PPG signal. The MA component generated by body motion (i.e. ACC-X and ACC-Y) is added to the PPG signal thereby affecting the accuracy of the HR estimation and this can be visualized from Fig. 3a. To overcome this issue, the proposed de-noising technique is used.

The PPG signal obtained after pre-processing is an appropriate input signal to the first stage of cascaded RLS filter. The noise signal ACC-X, is the reference input. In the proposed cascaded adaptive filter structure, the output from the first stage of RLS adaptive filter is a PPG signal with MA generated under the influence of ACC-X being diminished. The output of the first stage of RLS adaptive filter is a desired input signal to the second stage of RLS adaptive filter and ACC-Y, is the reference noise signal given as an input to the second stage. The second stage output of RLS adaptive filter is a PPG signal, where MA elements developed due to the ACC-Y is removed and the signal is provided as an input to the third stage of RLS adaptive filter. The accelerometer that records the body movements in *Z*-axis (ACC-Z), is the reference noise input to the third stage and its outcome is MA reduced PPG signal. This procedure is repeated for the NLMS and LMS based cascaded adaptive filter structures as shown in Fig. 2. The output at the third stage of each adaptive filter $s_{13}[n]$, $s_{23}[n]$ and $s_{33}[n]$ is a MA reduced PPG signal. These three PPG signals are combined to develop a MA reduced PPG signal $s[n]$, at the combinational layer C_{01} using the convex combination technique (i.e. softmax activation function) from which the HR is calculated as:

$$s[n] = \lambda_1[n]s_{13}[n] + \lambda_2[n]s_{23}[n] + \lambda_3[n]s_{33}[n] \quad (2)$$

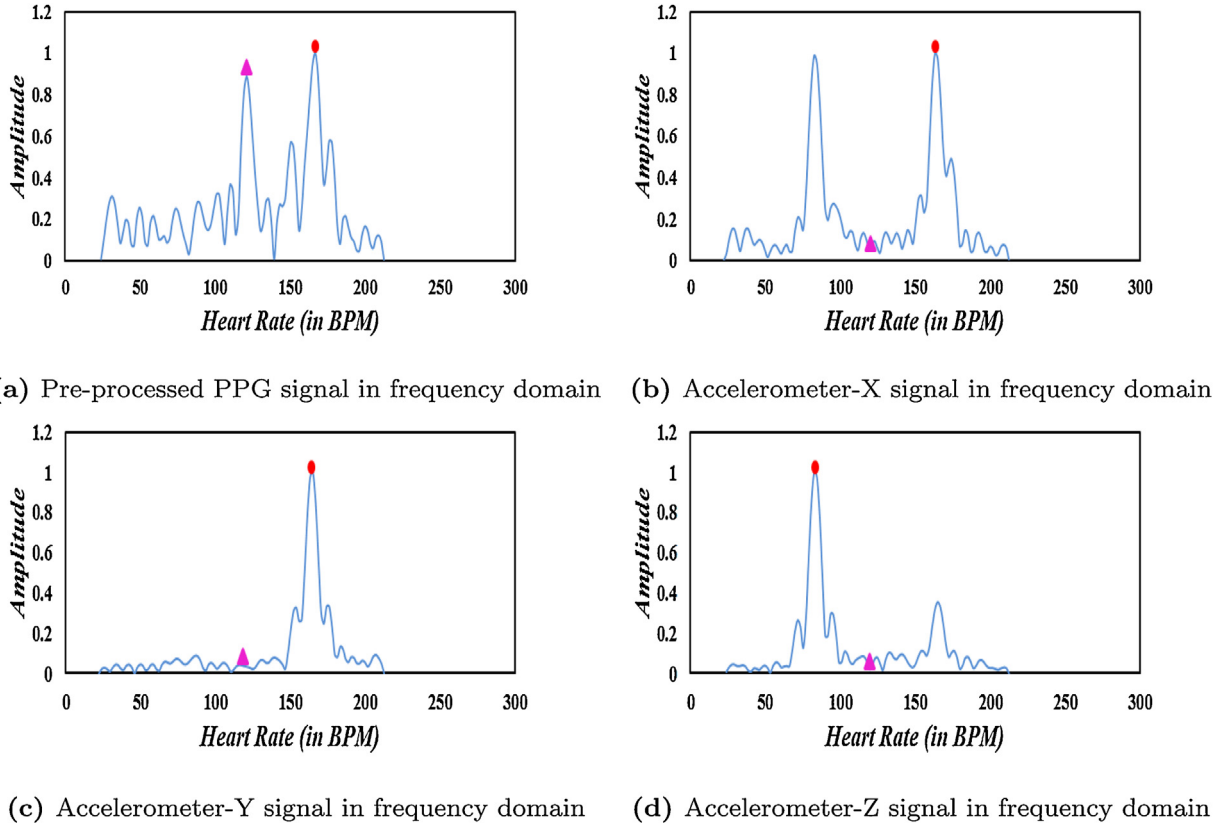

Fig. 3. Frequency domain representation of corrupted PPG and tri-axes accelerometer signals.

where $\lambda_1[n]$, $\lambda_2[n]$, $\lambda_3[n]$ – combinational parameters, $s_{13}[n]$ – MA reduced PPG signal using the cascaded RLS filter, $s_{23}[n]$ – MA reduced PPG signal using the cascaded NLMS filter, $s_{33}[n]$ – MA reduced PPG signal using the cascaded LMS filter, and $s[n]$ – MA reduced PPG signal.

The combinational parameters $\lambda_1[n]$, $\lambda_2[n]$ and $\lambda_3[n]$ are updated at each iteration. The parameters $a_1[n]$, $a_2[n]$ and $a_3[n]$ used in this algorithm that updates the values of $\lambda_1[n]$, $\lambda_2[n]$ and $\lambda_3[n]$ using the softmax activation function. The $\lambda_1[n]$, $\lambda_2[n]$ and $\lambda_3[n]$ are updated individually thereby all the combinational parameters remain positive and the sum of these combinational parameters should be one, i.e. $\lambda_1[n]+\lambda_2[n]+\lambda_3[n]=1$.

The values of $\lambda_1[n]$, $\lambda_2[n]$ and $\lambda_3[n]$ are updated at each iteration and it is given as:

$$\lambda_1[n] = \frac{e^{a_1[n]}}{e^{a_1[n]} + e^{a_2[n]} + e^{a_3[n]}} \tag{3}$$

$$\lambda_2[n] = \frac{e^{a_2[n]}}{e^{a_1[n]} + e^{a_2[n]} + e^{a_3[n]}} \tag{4}$$

$$\lambda_3[n] = \frac{e^{a_3[n]}}{e^{a_1[n]} + e^{a_2[n]} + e^{a_3[n]}} \tag{5}$$

$a_1[n]$, $a_2[n]$ and $a_3[n]$, that update the values of $\lambda_1[n]$, $\lambda_2[n]$ and $\lambda_3[n]$ at each iteration is given as:

$$a_1[n+1] = a_1[n] + \mu_{a1}(s_{13}[n] - s[n])s_{13}[n]\lambda_1[n](1-\lambda_1[n]) \tag{6}$$

$$a_2[n+1] = a_2[n] + \mu_{a2}(s_{13}[n] - s[n])s_{23}[n]\lambda_2[n](1-\lambda_2[n]) \tag{7}$$

$$a_3[n+1] = a_3[n] + \mu_{a3}(s_{13}[n] - s[n])s_{33}[n]\lambda_3[n](1-\lambda_3[n]) \tag{8}$$

where μ_{a1}, μ_{a2}, μ_{a3} – step size parameters.

Algorithm 1. Algorithm for updating the combinational parameters $\lambda_1[n]$, $\lambda_2[n]$, and $\lambda_3[n]$

Initialize: $\lambda_1[1]=0.5$, $\lambda_2[1]=0.25$, $\lambda_3[1]=0.25$, $a_1[1]=0$, $a_2[1]=0$, $a_3[1]=0$, $\mu_{a1}=0.5$, $\mu_{a2}=0.5$, $\mu_{a3}=0.5$.
for $n=1$ to 1000 **do**
$s[n] = \lambda_1[n]s_{13}[n] + \lambda_2[n]s_{23}[n] + \lambda_3[n]s_{33}[n]$
$e_1[n] = s_{13}[n] - s[n]$
$a_1[n+1] = a_1[n] + \mu_{a1}e_1[n]s_{13}[n]\lambda_1[n](1-\lambda_1[n])$
$a_2[n+1] = a_2[n] + \mu_{a2}e_1[n]s_{23}[n]\lambda_2[n](1-\lambda_2[n])$
$a_3[n+1] = a_3[n] + \mu_{a3}e_1[n]s_{33}[n]\lambda_3[n](1-\lambda_3[n])$
$\lambda_1[n+1] = \frac{e^{a_1[n]}}{e^{a_1[n]}+e^{a_2[n]}+e^{a_3[n]}}$
$\lambda_2[n+1] = \frac{e^{a_2[n]}}{e^{a_1[n]}+e^{a_2[n]}+e^{a_3[n]}}$
$\lambda_3[n+1] = \frac{e^{a_3[n]}}{e^{a_1[n]}+e^{a_2[n]}+e^{a_3[n]}}$
end for

2.2.3. HR estimation & tracking

The HR is estimated from the MA reduced PPG signal, $s[n]$ using the periodogram. The formula used to estimate the HR is as given below:

$$HR_{init}(k) = loc \times 60 \times \frac{F_s}{N} \tag{9}$$

where loc – highest spectral peak's location and $HR_{init}(k)$ – kth window's initial heart rate value (in BPM) estimated from the de-noised PPG signal, F_s – sampling frequency (125 Hz), N – total FFT points ($N=4096$).

Fig. 4 depicts the HR estimation from the corrupted PPG signals. The periodogram of the PPG signal before MA removal is plotted and the HR is estimated using Eq. (9). The red circle symbolizes the estimated HR and the pink triangle symbolizes the original HR. The periodogram of accelerometer signals are shown in Fig. 4b–d gives an idea about the HR values having strong MA component which in turn probably corrupts the PPG signal at these HR values. The periodogram of the de-noised PPG signal depicted in Fig. 4d, indicates that the estimated HR and the actual HR are same. This clearly states that the proposed method is an efficient de-noising technique.

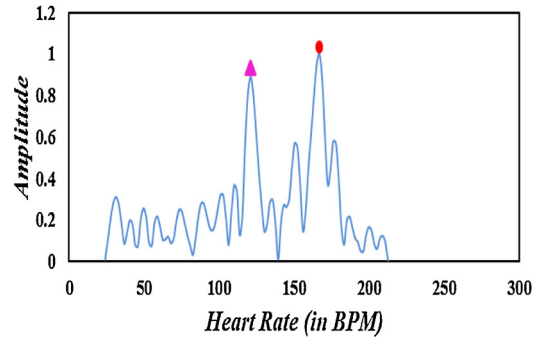

(a) Pre-processed PPG signal in frequency domain

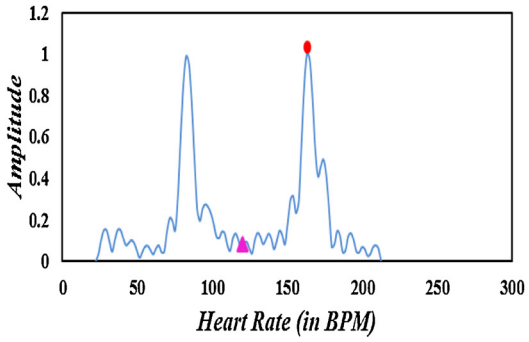

(b) Accelerometer-X signal in frequency domain

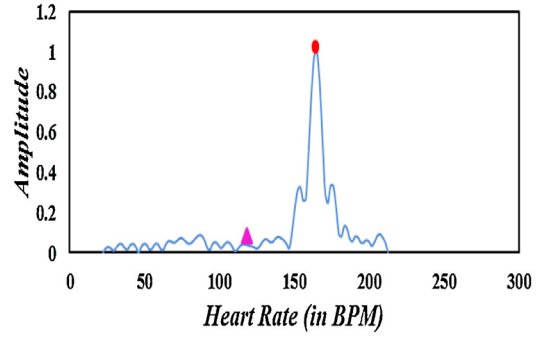

(c) Accelerometer-Y signal in frequency domain

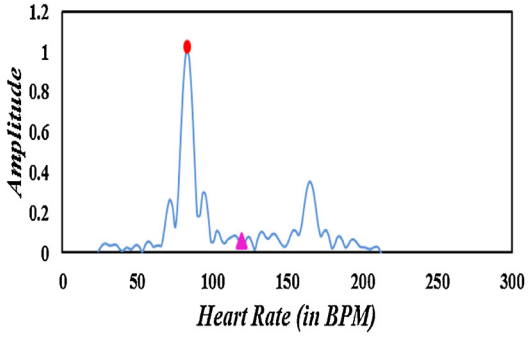

(d) Accelerometer-Z signal in frequency domain

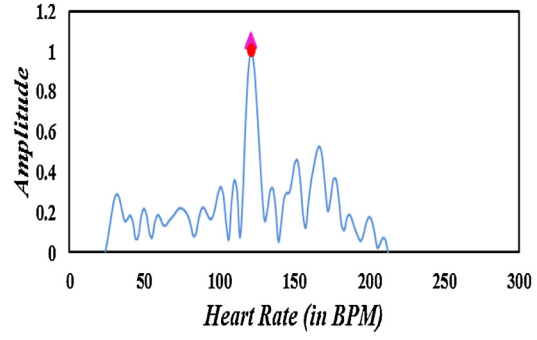

(e) MA reduced PPG signal in frequency domain

Fig. 4. HR estimation from the corrupted PPG signals.

There are some cases where the HR estimated using Eq. (9) do not match with the HR obtained from ECG. This may occur due to the absence of the highest peak in the expected location or due to the change in the location of the highest peak. This scenario is clearly illustrated in Fig. 5. Even after de-noising, there are chances for the estimated HR (red circle) to deviate from the original HR (pink triangle) which is shown in Fig. 5e.

To counterbalance the issue of inaccurate HR estimation, HR tracking technique is implemented. The HR value estimated is expected to change gradually with reference to the previous window's HR. This is because of the fact that out of 1000 samples used to estimate the HR of each PPG signal window, the 750 samples at the end of the previous PPG signal is the first 750 samples in the current PPG signal window to which new 250 samples are concatenated and this pattern is repeated. This triggered the idea of developing a concept called 'Search Range' (SR). The SR uses the highest peak's location (i.e. HR) of the previous MA reduced PPG signal (N_{prev}), as a reference to select the HR of the current PPG signal. The search range is represented as

$$SR = \left[N_{prev} - \Delta, N_{prev} + \Delta\right] \tag{10}$$

where Δ – constant and it is assigned a value of 10 for the first 15 PPG signal windows (≈30 s) in each recordings and later it is updated adaptively based on the power value of the accelerometer signals. If the power of the accelerometer signals is less than the power of PPG signal by 75%, then the Δ is the maximum difference value of the previous 15 HR values estimated and if the power of the accelerometer signals is not less than the power of the PPG signal by 75%, then the Δ is the maximum difference value of the previous 10 HR values estimated. After deciding the SR, the HR estimated from tracking is given as

$$HR_{SR}(k) = loc_{SR} \times 60 \times \frac{F_s}{N} \tag{11}$$

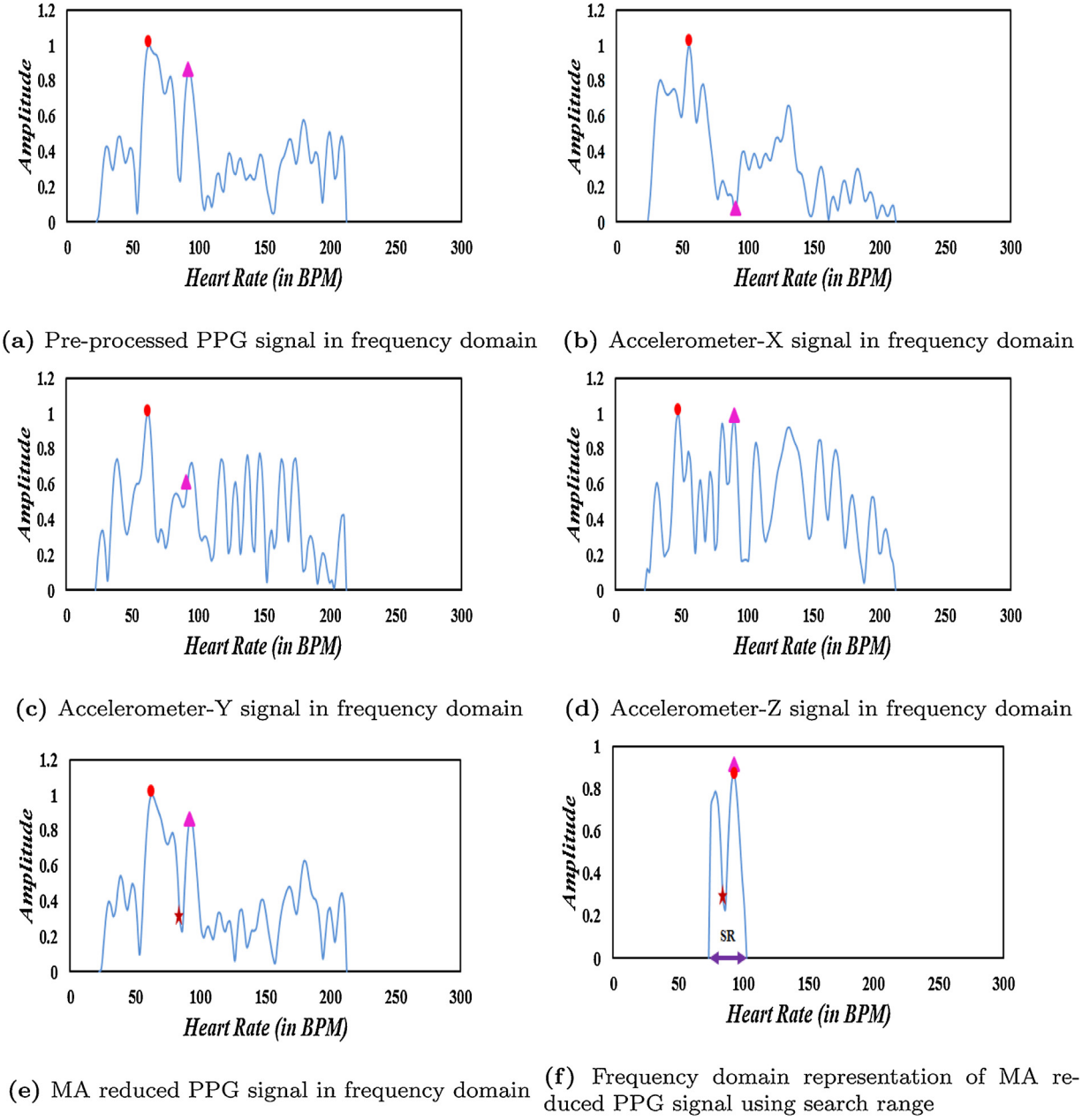

(a) Pre-processed PPG signal in frequency domain (b) Accelerometer-X signal in frequency domain

(c) Accelerometer-Y signal in frequency domain (d) Accelerometer-Z signal in frequency domain

(e) MA reduced PPG signal in frequency domain (f) Frequency domain representation of MA reduced PPG signal using search range

Fig. 5. Effect of search range in HR estimation.

where loc_{SR} – highest spectral peak's location within the search range and $HR_{SR}(k)$ – kth window's initial heart rate value (in BPM) estimated from the search range.

Instead of evaluating multiple peaks to estimate HR from an entire de-noised signal, the location within the *SR* at which the highest peak value occurred is considered as HR of the current window as shown in Fig. 5f. This ensured the reduction in the computational time. Due to the reduction in the computational complexity, the HR estimated from tracking alone is highly significant and it plays a major role in HR estimation. Tracking leads to an accurate estimation of HR and it is shown in Fig. 5f. A brown star in Fig. 5e and f represents the HR of the previous MA reduced PPG signal, $HR_{est}(k-1)$. The location of the highest peak of the previous PPG signal, (N_{prev}), is same as the previous PPG signal's loc_{SR}. In Fig. 5f, the HR estimated from the previous de-noised PPG signal, $HR_{est}(k-1)$, represented by a brown star is approximately 82 BPM and the value of (N_{prev}) is 45. The value of Δ assigned is 10 and the maximum peak within the search range [45 – 10, 45 + 10], i.e. 35–55 location points are considered for estimating the HR. The HR estimated should be between 64 and 100 BPM, i.e. $35 \times 60 \times \frac{125}{4096}$ to $55 \times 60 \times \frac{125}{4096}$ using Eq. (11).

The phase vocoder is used to fine tune the HR estimate, $(HR_{SR}(k))$, by estimating the instantaneous frequency (in BPM). The instantaneous frequency is calculated as a discrete derivative of the phase, which uses the phase information of the present and previous PPG signal windows that were obtained from the polar representation of the FFT. The phase information of the present and previous PPG signal windows of the selected frequency having the maximum peak value in the magnitude spectrum is used to improve the initial HR. The series, $\bar{HR}_{pv}(n)$, is computed for different values of n using Eq. (12), and the value of $\bar{HR}_{pv}(n)$ which is nearest to the initial HR,

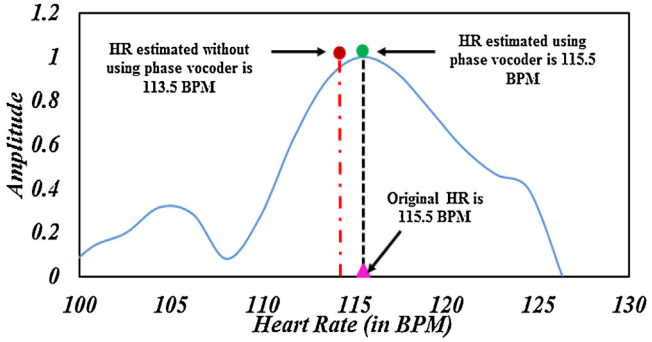

Fig. 6. Effect of phase vocoder in fine tuning the HR.

estimated using Eq. (11), is chosen as the HR. The instantaneous frequency is given as

$$\overline{HR}_{pv}(n) = \frac{\Theta_2 - \Theta_1 + 2\pi n}{2\pi(t_2 - t_1)} \times 60 \tag{12}$$

$$HR_{est}(k) = \underset{n}{arg\,min}(\overline{HR}_{pv}(n) - HR_{SR}(k)) \tag{13}$$

where Θ_2, Θ_1 – phase information of the present and previous PPG signal windows, n – is an integer (n varies from 1 to 20; in this case), t_2 & t_1 – time stamps of the present and previous PPG windows, $(t_2 - t_1 = 2\,s)$ (i.e. window shift).

The effect of phase vocoder in fine tuning the HR is clearly illustrated in Fig. 6. After de-noising, HR (in BPM) of the PPG signal is estimated by taking the FFT, and the HR (in BPM) having the maximum peak in the magnitude spectrum is indicated by a marron circle and red dotted line represents the corresponding HR. The HR is estimated as 113.5 BPM. The HR obtained from ECG is 115.5 BPM and it is represented by a pink triangle. Similarly, by involving phase vocoder, the HR (in BPM) having the maximum peak in the magnitude spectrum is represented by a green circle and black colored dotted line represents the corresponding HR of PPG signal after fine tuning. The HR estimated using the phase vocoder is 115.5 BPM and it is same as the HR of the ECG signal.

2.3. Post-processing

Using the linear regression method, the final HR is obtained by taking the weighted average of the estimated HR and the predicted HR. If the difference between any two consecutive HR values exceeds 5 BPM, then HR prediction is used as given below:

$$HR_{est}(k) = \alpha HR_{est}(k) + (1 - \alpha) HR_{LinReg} \tag{14}$$

where HR_{LinReg} – prediction obtained from the regression line that is fitted over the previous six windows HR value using least square error with α at 0.75.

3. Experimental results

3.1. Metrics and result evaluation

The accuracy of the proposed algorithm is examined by the metric, absolute error (AE), which is the difference between the HR estimated from both PPG and the ECG signals. Average Error is calculated from the formula given as,

$$AE(k) = \left| HR_{est}(k) - HR_{true}(k) \right| \tag{15}$$

The average absolute error (μ_{AE}), standard deviation of the absolute error (σ_{AE}) and average of the relative error ($\bar{e}_{RE}$) are the overall metrics calculated using the formula given in (16)–(18):

$$\mu_{AE} = \frac{1}{w}\sum_{k=1}^{w} |HR_{est}(k) - HR_{true}(k)| \tag{16}$$

$$\sigma_{AE} = \sqrt{\frac{1}{w}\sum_{k=1}^{w} (AE(k) - \mu_{AE})^2} \tag{17}$$

$$\bar{e}_{RE} = \frac{1}{w}\sum_{k=1}^{w} \frac{AE(k)}{HR_{true}(k)} \tag{18}$$

where w – total number of windows used.

Table 1 compares μ_{AE} values estimated using the proposed technique with the other existing methods for all 22 PPG datasets. The

Table 1
Comparison of μ_{AE} values estimated using proposed technique with other existing methods for 22 PPG datasets.

Data set	Exercise type	Overall metrics	Troika [12]	JOSS [13]	TEMKO [14]	GALLI [17]	A.K.R. [29]	Proposed work
1	T1		2.29	1.33	1.25	2.72	1.34	1.13
2	T1		2.19	1.75	1.41	3.25	0.70	0.87
3	T1		2.00	1.47	0.71	1.40	0.66	0.73
4	T1		2.15	1.48	0.97	1.21	0.70	0.95
5	T1		2.01	0.69	0.75	0.93	0.63	0.85
6	T1		2.76	1.32	0.92	2.12	0.86	0.94
7	T1		1.67	0.71	0.65	1.40	0.66	0.66
8	T1		1.93	0.56	0.97	1.16	0.58	0.70
9	T1		1.86	0.49	0.55	1.17	0.52	0.59
10	T1		4.70	3.81	2.06	4.14	2.46	3.94
11	T1		1.72	0.78	1.03	1.38	1.21	1.01
12	T1		2.84	1.04	0.99	1.29	0.74	0.95
13	T2		6.63	8.07	9.59	9.59	14.40	12.16
14	T2		1.94	1.61	2.57	3.65	1.45	1.42
15	T3		7.82	3.10	2.25	3.90	11.47	2.05
16	T3		2.46	7.01	3.01	2.44	4.80	2.67
17	T3		1.73	2.99	2.73	2.14	1.51	1.45
18	T3		3.33	1.67	1.57	2.60	8.21	1.37
19	T2		2.69	2.80	2.10	1.86	4.65	1.74
20	T3		0.51	1.88	3.44	0.85	10.54	3.18
21	T3		1.35	0.92	1.61	3.06	0.84	1.06
22	T2		3.41	0.49	0.75	3.38	0.68	0.59
Mean (1–22)		μ_{AE}	2.73	2.08	1.90	2.45	3.16	**1.86**
		σ_{AE}	2.99	2.79	2.37	2.83	4.65	**2.36**
		$\bar{e}_{RE}$	2.33	1.91	1.98	2.21	2.80	**1.77**

T1 = running activity performed using treadmill. T2 = exercises for arm recovery. T3 = fast arm swing.

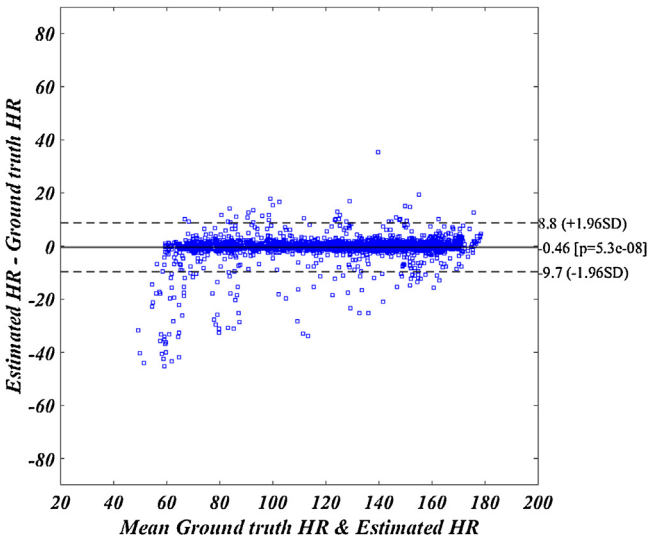

Fig. 7. Bland–Altman plot for 22 PPG dataset.

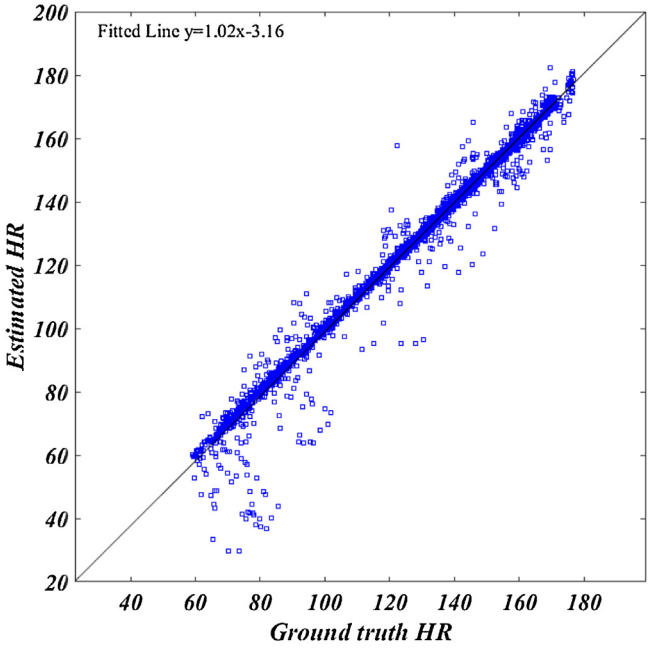

Fig. 8. Scatter plot for 22 PPG dataset.

overall metrics calculated using the proposed technique are less when compared with other methods as tabulated in Table 1. The performance of the proposed method is considerably good and it resulted in μ_{AE} of 1.86. The reported μ_{AE} is less compared with other existing methods. Pearson correlation is a measure of similarities between the available ECG based HR and the HR estimated from the PPG signal. The Pearson correlation is 0.9880. The μ_{AE} obtained using the proposed method is 1.86 ± 2.36 BPM (mean $\pm$ std. deviation) for the 22 PPG datasets (12 training datasets and 10 test datasets).

The Bland–Altman graph plotted in Fig. 7, is the agreement between the HR of PPG and ECG. The scatter plot shown in Fig. 8, is a plot between the ECG's HR and the PPG's HR over the 22 datasets. The Limit of Agreement (LoA) is $[-9.7, 8.8]$ BPM. The plot between

Table 2
Comparison of timing analysis.

S. no.	De-noising technique	Mean (1–22)	Computational time (in seconds)
1	Hierarchical structure [29]	3.16	43.22
2	Proposed method	1.86	**32.19**

The bold value specify the values obtained by the proposed technique and it is less compared to other state of art methods.

the original HR and estimated HR values (i.e. Scatter plot) over the entire 22 datasets is shown in Fig. 8.

3.2. Parameter values

The step size of 0.0005 and 0.0001 are assigned to NLMS and LMS adaptive filters. The order of the adaptive filters are chosen based on the experimental analysis and also from the literature. Filter order of 26 is used for NLMS as well as for LMS adaptive filters and the filter order of 54 is preferred for RLS adaptive filter as in [29].

3.3. Timing analysis

The combination of adaptive filters results in efficient de-noising but at the cost of increased computational time. There is always a trade-off between the accuracy (error) and computational time. The proposed de-noising method resulted in a better accuracy with a reduction in computational time when compared with another de-noising structure that used the combination of adaptive filters [29]. The mean computational time for 1–22 PPG dataset is calculated from Matlab R 2017a. The timing analysis of the proposed de-noising method and hierarchical structure has been done on Intel core i7-4770 processor at 3.40 GHz and is given in Table 2 below:

4. Conclusion

A robust HR estimation method for the removal of MA components from the PPG signals using an efficient de-noising technique that combines cascaded structure of RLS, NLMS and LMS adaptive filters has been proposed. The method that has been proposed is evaluated using 22 datasets performing different physical activity. It is noted that the HR estimated using the proposed de-noising method is accurate for the datasets that performed running activity on the treadmill, arm recovery exercise and fast arm movements. Future research may emphasize more on reducing the computational time and improving the accuracy still further, before developing a prototype of a wearable device using FPGA.

Acknowledgement

The authors would like to thank MeitY (Ministry of Electronics and Information Technology), Government of India, for the financial assistance (PhD-MLA/4(16)/2015-16).

Conflict of interest: The authors declare that they have no conflict of interest.

References

[1] J. Allen, Photoplethysmography and its application in clinical physiological measurement, Physiol. Meas. 28 (3) (2007) R1.
[2] K.-c. Lan, P. Raknim, W.-F. Kao, J.-H. Huang, Toward hypertension prediction based on PPG-derived HRV signals: a feasibility study, J. Med. Syst. 42 (6) (2018) 103.

[3] C.E. King, M. Sarrafzadeh, A survey of smartwatches in remote health monitoring, J. Healthc. Informat. Res. (2017) 1–24.
[4] B. Sun, Z. Zhang, Photoplethysmography-based heart rate monitoring using asymmetric least squares spectrum subtraction and Bayesian decision theory, IEEE Sens. J. 15 (12) (2015) 7161–7168.
[5] D. Zhao, Y. Sun, S. Wan, F. Wang, SFST: a robust framework for heart rate monitoring from photoplethysmography signals during physical activities, Biomed. Signal Process. Control 33 (2017) 316–324.
[6] E. Khan, F. Al Hossain, S.Z. Uddin, S.K. Alam, M.K. Hasan, A robust heart rate monitoring scheme using photoplethysmographic signals corrupted by intense motion artifacts, IEEE Trans. Biomed. Eng. 63 (3) (2016) 550–562.
[7] R. Yousefi, M. Nourani, S. Ostadabbas, I. Panahi, A motion-tolerant adaptive algorithm for wearable photoplethysmographic biosensors, IEEE J. Biomed. Health Informat. 18 (2) (2014) 670–681.
[8] H. Dubey, R. Kumaresan, K. Mankodiya, Harmonic sum-based method for heart rate estimation using PPG signals affected with motion artifacts, J. Amb. Intell. Hum. Comput. 9 (1) (2018) 137–150.
[9] S.H. Kim, D.W. Ryoo, C. Bae, Adaptive noise cancellation using accelerometers for the PPG signal from forehead, 29th Annual International Conference of the IEEE Engineering in Medicine and Biology Society, 2007, EMBS 2007 (2007).
[10] H. Lee, H. Chung, H. Ko, J. Lee, Wearable multichannel photoplethysmography framework for heart rate monitoring during intensive exercise, IEEE Sens. J. 18 (7) (2018) 2983–2993.
[11] Y. Fujita, M. Hiromoto, T. Sato, Parhelia: particle filter-based heart rate estimation from photoplethysmographic signals during physical exercise, IEEE Trans. Biomed. Eng. 65 (1) (2018) 189–198.
[12] Z. Zhang, Z. Pi, B. Liu, Troika: a general framework for heart rate monitoring using wrist-type photoplethysmographic signals during intensive physical exercise, IEEE Trans. Biomed. Eng. 62 (2) (2015) 522–531.
[13] Z. Zhang, Photoplethysmography-based heart rate monitoring in physical activities via joint sparse spectrum reconstruction, IEEE Trans. Biomed. Eng. 62 (8) (2015) 1902–1910.
[14] A. Temko, Accurate heart rate monitoring during physical exercises using PPG, IEEE Trans. Biomed. Eng. 64 (9) (2017) 2016–2024.
[15] M.A. Motin, C.K. Karmakar, M. Palaniswami, PPG derived heart rate estimation during intensive physical exercise, IEEE Access 7 (2019) 56062–56069.
[16] B. Lee, J. Han, H.J. Baek, J.H. Shin, K.S. Park, W.J. Yi, Improved elimination of motion artifacts from a photoplethysmographic signal using a Kalman smoother with simultaneous accelerometry, Physiol. Meas. 31 (12) (2010) 1585.
[17] A. Galli, C. Narduzzi, G. Giorgi, Measuring heart rate during physical exercise by subspace decomposition and Kalman smoothing, IEEE Trans. Instrum. Meas. (2017).
[18] S.S. Haykin, Adaptive Filter Theory, Pearson Education India, 2008.
[19] M.-Z. Poh, N.C. Swenson, R.W. Picard, Motion-tolerant magnetic earring sensor and wireless earpiece for wearable photoplethysmography, IEEE Trans. Inform. Technol. Biomed. 14 (3) (2010) 786–794.
[20] B. Widrow, J.R. Glover, J.M. McCool, J. Kaunitz, C.S. Williams, R.H. Hearn, J.R. Zeidler, J.E. Dong, R.C. Goodlin, Adaptive noise cancelling: principles and applications, Proc. IEEE 63 (12) (1975) 1692–1716.
[21] T. Schäck, C. Sledz, M. Muma, A.M. Zoubir, A new method for heart rate monitoring during physical exercise using photoplethysmographic signals, 2015 23rd European Signal Processing Conference (EUSIPCO) (2015) 2666–2670.
[22] S.S. Chowdhury, R. Hyder, M.S.B. Hafiz, M.A. Haque, Real-time robust heart rate estimation from wrist-type PPG signals using multiple reference adaptive noise cancellation, IEEE J. Biomed. Health Informat. 22 (2) (2018) 450–459.
[23] M.T. Islam, I. Zabir, S.T. Ahamed, M.T. Yasar, C. Shahnaz, S.A. Fattah, A time-frequency domain approach of heart rate estimation from photoplethysmographic (PPG) signal, Biomed. Signal Process. Control 36 (2017) 146–154.
[24] Y. Ye, Y. Cheng, W. He, M. Hou, Z. Zhang, Combining nonlinear adaptive filtering and signal decomposition for motion artifact removal in wearable photoplethysmography, IEEE Sens. J. 16 (19) (2016) 7133–7141.
[25] M.S. Islam, M. Shifat-E-Rabbi, A.M.A. Dobaie, M.K. Hasan, Preheat: precision heart rate monitoring from intense motion artifact corrupted PPG signals using constrained RLS and wavelets, Biomed. Signal Process. Control 38 (2017) 212–223.
[26] J. Arenas-García, A.R. Figueiras-Vidal, A.H. Sayed, Mean-square performance of a convex combination of two adaptive filters, IEEE Trans. Signal Process. 54 (3) (2006) 1078–1090.
[27] J. Arenas-Garcia, L.A. Azpicueta-Ruiz, M.T. Silva, V.H. Nascimento, A.H. Sayed, Combinations of adaptive filters: performance and convergence properties, IEEE Signal Process. Mag. 33 (1) (2016) 120–140.
[28] K.R. Arunkumar, R. Srivathsa, M. Bhaskar, Improved heart rate estimation from photoplethysmography during physical exercise using combination of NLMS and RLS adaptive filters, IEEE Region 10 Conference TENCON 2018 (2018) 0420–0424.
[29] K.R. Arunkumar, M. Bhaskar, Heart rate estimation from photoplethysmography signal for wearable health monitoring devices, Biomed. Signal Process. Control 50 (2019) 1–9.
[30] Y. Zhang, B. Liu, Z. Zhang, Combining ensemble empirical mode decomposition with spectrum subtraction technique for heart rate monitoring using wrist-type photoplethysmography, Biomed. Signal Process. Control 21 (2015) 119–125.